Chemosphere 144 (2016) 285–291

Contents lists available at ScienceDirect

Chemosphere

journal homepage: www.elsevier.com/locate/chemosphere

Sorption of four hydrophobic organic contaminants by biochars derived from maize straw, wood dust and swine manure at different pyrolytic temperatures

Ziying Wang[a], Lanfang Han[a], Ke Sun[a,*], Jie Jin[a], Kyoung S. Ro[b], Judy A. Libra[c], Xitao Liu[a], Baoshan Xing[d]

[a] State Key Laboratory of Water Environment Simulation, School of Environment, Beijing Normal University, Beijing, 100875, China
[b] Coastal Plains Soil, Water, and Plant Research Center, Agricultural Research Service, U.S. Department of Agriculture, 2611 West Lucas Street, Florence, SC, 29501, USA
[c] Leibniz Institute for Agricultural Engineering, Max-Eyth-Allee 100, 14469 Potsdam-Bornim, Germany
[d] Stockbridge School of Agriculture, University of Massachusetts, Amherst, MA, 01003, USA

HIGHLIGHTS

- Swine manure biochars had higher sorption capacity, due to its higher ash content.
- Pore filling could dominate the sorption of tested biochars.
- Surface polarity and aliphatic C affect sorption of low temperature wood biochars.
- Aromatic C may regulate the sorption of biochars produced at high temperatures.

ARTICLE INFO

Article history:
Received 1 February 2015
Received in revised form 21 July 2015
Accepted 11 August 2015
Available online 10 September 2015

Handling editor: Xinde Cao

Keywords:
Biochar
CO_2-surface area
Surface polarity
Sorption
Minerals

ABSTRACT

Sorption behavior of acetochlor (ACE), dibutyl phthalate (DBP), 17α-Ethynyl estradiol (EE2) and phenanthrene (PHE) with biochars produced from three feedstocks (maize straw (MABs), pine wood dust (WDBs) and swine manure (SWBs)) at seven heat treatment temperatures (HTTs) was evaluated. The bulk polarity of these biochars declined with increasing HTT while the aromaticity and CO_2-surface area (CO_2-SA) rose. The surface OC contents of biochars were generally higher than bulk OC contents. The organic carbon (OC)-normalized CO_2-SA (CO_2-SA/OC) of biochars significantly correlated with the sorption coefficients (n and $\log K_{oc}$), suggesting that pore filling could dominate the sorption of tested sorbates. SWBs had higher $\log K_{oc}$ values compared to MABs and WDBs, due to their higher ash contents. Additionally, the $\log K_{oc}$ values for MABs was relatively greater than that for WDBs at low HTTs ($\leq$400 °C), probably resulting from the higher CO_2-SA/OC, ash contents and aromaticity of MABs. Surface polarity and the aliphatic C may dominate the sorption of WDBs obtained at relatively low HTTs ($\leq$400 °C), while aromatic C affects the sorption of biochars at high HTTs. Results of this work aid to deepen our understanding of the sorption mechanisms, which is pivotal to wise utilization of biochars as sorbents for hazardous organic compounds.

1. Introduction

Biochars, which are products of the pyrolytic processing of biomass materials (Chun et al., 2004; Chen et al., 2008), has attracted increasing interest since their application to soil could act as effective sorbents for organic pollutants (Chun et al., 2004; Chen et al., 2008), may enhance the sequestration of atmospheric carbon dioxide (Lehmann et al., 2006), and simultaneously improve soil fertility (Sohi et al., 2010). Studies have shown that the physiochemical properties of biochars, which would govern their sorption capacity for hydrophobic organic compounds (HOCs) (Chen et al., 2008; Sun et al., 2011a, 2012), vary remarkable with feedstock sources and pyrolysis process conditions, among which heat treatment temperature (HTT) is a key factor (Chen et al., 2008; Keiluweit et al., 2010; Sun et al., 2012). Generally, biochars produced at lower HTTs (250–400 °C) are not fully carbonized, but have higher yields and contain more diversified organic structures, including aliphatic and cellulose structures (Novak et al., 2009). While those made at relatively high HTTs (400–700 °C) are well

* Corresponding author.
E-mail address: sunke@bnu.edu.cn (K. Sun).

http://dx.doi.org/10.1016/j.chemosphere.2015.08.042
0045-6535/

carbonized with large amounts of condensed aromatic C structures (Keiluweit et al., 2010) and exhibit rigid surfaces along with considerable pores for nonlinear adsorption of HOCs (Chen et al., 2008, 2012; Sun et al., 2011a). The question on how these different physiochemical properties can be correlated to the difference in sorption capacity for HOCs has been the subject of much recent work.

For biochars produced at various HTTs from chitin and cellulose, the sorption capacity (e.g., organic carbon (OC)-normalized distribution coefficient (K_{oc})) for phenanthrene (PHE) and naphthalene (NAPH) was enhanced as the aromatic domains and surface area (SA) of the chars increased with increasing HTTs (Wang and Xing, 2007). In contrast, the sorption of polar phthalic acid esters (PAEs) was found to be controlled by the aliphatic and polar domains within biochars derived from both high and low HTTs (Sun et al., 2012). Furthermore, there is emerging evidence to indicate that chars appeared to have a higher surface capacity for a polar sorbate than for a nonpolar sorbate (Chun et al., 2004; Sun et al., 2012). Based on these, it can be reasonably assumed that due to the hydrophobicity and structure difference of sorbates, dissimilar sorption mechanisms would take place between different sorbates and biochars. Moreover, with respect to the same sorbate, sorption mechanisms also possibly vary with the HTT at which biochars were produced. In order to systematically probe the mechanism underlying the interactions between HOCs and biochars, biochars produced at a set of HTTs were used as sorbents, acetochlor (ACE), dibutyl phthalate (DBP), 17α-Ethynyl estradiol (EE2) and PHE were selected as sorbates owing to their different polarity, element composition, electron polarizability and aromaticity.

A recent study found that minerals within biochars may exert an influence upon the organic matter (OM) spatial arrangement within biochars, thereby influencing the sorption of HOCs by biochars (Sun et al., 2013). While the focus of most current studies has been on sorption with low-mineral plant residue-derived biochars (PLABs), the sorption properties of high-mineral animal waste-derived biochar (ANIBs) have rarely been investigated. Therefore, it is necessary to further probe the characteristics of high-mineral biochars along with their sorption behavior.

Thus, the major works of this study were to 1) systematically examine the bulk and surface characteristics of biochars produced from feedstock materials with different mineral levels, including the maize straw, pine sawdust and swine manure at different HTTs; 2) investigate the sorption characteristics of ACE, DBP, EE2 and PHE by tested biochars; and 3) further test the roles of biochars characteristics (i.e., minerals, polarity, aromaticity and SA) in HOCs sorption.

2. Materials and methods

2.1. Sorbates

ACE (98 + %), a non-ionic and non-volatile herbicide, and DBP (99 + %), one of the most widely used PAEs, were purchased from Dr. Ehrenstorfer GmbH (Augsburg, Germany). EE2 (98 + %), one of the most frequently studied endocrine disrupting chemicals (EDCs) in environmental research, was obtained from Aldrich Co. (Milwaukee, WI). PHE (98 + %), which is a ubiquitous polycyclic aromatic hydrocarbon (PAHs) in the environment, was purchased from Sigma–Aldrich Chemical Co. Selected physicochemical properties of ACE, DBP, EE2 and PHE are presented in Table S1, Supplementary data.

2.2. Sorbents

The specific processes of biochar preparation were reported in a previous study (Sun et al., 2013). Briefly, maize straw (Henan Province, China), pine sawdust (Heilongjiang Province, China) and dewatered swine manure (Beijing, China) samples were obtained and air-dried at room temperature. Maize straw and pine wood dust were washed with deionized water (DI water) before use. Then all dried feedstock materials were ground to obtain a particle size of less than 1.5 mm and then pyrolyzed for 1 h at seven HTTs (i.e., 250, 300, 350, 400, 450, 500, and 600 °C) under oxygen-limited conditions in a muffle furnace. Next, the biochars were treated with 0.1 M HCl to decrease pH values of biochars and remove some nutrients (soluble salts and potassium compounds), carbonates, and dissolved organic matter (DOM) as well, which could prevent other factors mainly including pH values and DOM of biochars from impacting HOCs sorption by biochars. After the supernatants were removed by centrifugation, the residues were washed with DI water until the aqueous phase became nearly neutral and then dried at 105 °C. Subsequently, the biochars were gently milled to pass a 0.25 mm sieve (60 meshes) for further analysis. According to their feedstocks and HTTs, the 21 biochars are hereafter referred to as: MAXXX (maize straw), WDXXX (pine wood dust) and SWXXX (swine manure), with XXX indicating the charring temperature (250–600 °C). For comparison, samples of the feedstock, MA0, WD0 and SW0, were also analyzed. Here, the biochars were classified to PLABs (maize biochars (MABs) and wood dust biochars (WDBs)) and ANIBs (swine biochars (SWBs)) according to the feedstock sources. The biochars produced at low temperatures and high temperatures were named as LTBs and HTBs, respectively.

2.3. Biochar characterization

The bulk organic carbon (OC, the carbonate–free basis), H, N, and O contents of all the biochars were measured using an Elementar Vario ELIII elemental analyzer via complete combustion. Ash contents of the biochars were determined by heating samples at 750 °C for 4 h. To get more information on the chemical composition of biochars, solid-state cross-polarization magic angle spinning ^{13}C nuclear magnetic resonance (^{13}C NMR) spectra were obtained using a Bruker Avance 300 NMR spectrometer (Karlsruhe, Germany) operated at a ^{13}C frequency of 75 MHz and a magic angle spinning rate of 12 KHz. Surface area (CO_2-SA) using CO_2 isotherm at 273 K was detected by gas adsorption using an Autosorb-1 gas analyzer (Quantachorme Instrument Corp., Boynton Beach, FL) and calculated using nonlocal density functional theory (NLDFT) (Braida et al., 2003). The surface functionalities and domain spatial arrangement of samples were determined using X-ray photoelectron spectra (XPS) with a Kratos Axis Ultra electron spectrometer using monochromated Al Kα source operated at 225 W, and more detailed information of XPS characterization was described elsewhere (Yang et al., 2011; Sun et al., 2013). (The C_{1s} binding energy levels were assigned as following: 284.9 ev for C–C, 286.5 ev for C–O, 287.9 ev for C=O, and 289.4 ev for COO.)

2.4. Sorption experiments

The sorption isotherms were obtained by a batch equilibration of biochar samples in glass vials with Teflon-lied screw caps. For the sorption of ACE, 8 mL glass vials were used for all the sorbents; for DBP and EE2, 15 mL glass vials were used for biochars produced at 500 and 600 °C, and 8 mL glass vials for the rest sorbents; and for PHE, 8 mL were used for feedstock samples, 40 mL for the biochars produced at 250–350 °C, and the 60 mL for the rest sorbents. The background solution contained 0.01 M $CaCl_2$ to maintain a constant ionic strength and 200 mg/L NaN_3 as a biocide. The initial concentrations of test solutions ranged from 100 to 100,000 μg/L for ACE, from 100 to 6000 μg/L for DBP, from 50 to 3000 μg/L for EE2, and from 2 μg/L to 1000 μg/L for PHE, respectively. The sorption experiment was carried out on a rotary shaker

for 7 d (ACE, DBP and EE2) or 10 d (PHE) at 23 ± 1 °C. Our preliminary experiments showed that the time period was long enough to reach the sorption equilibration.

After all vials were placed upright for 24 h, the supernatant was transferred to a 2 mL vial for HPLC (reversed phase C18, 25 cm × 4.6 mm × 5 μm (ACE, DBP and PHE) or 15 cm × 4.6 mm × 5 μm (EE2)) analysis. ACE was analyzed with a UV detector at 222 nm. The mobile phase was 75:25 (v:v) of acetonitrile and deionized water and the flow rate was 1 mL/min. The concentration of DBP was determined by using an UV detector at 228 nm. The mobile phase was a mixture of 80:20 (v:v) of acetonitrile and deionized water and the flow rate was 1 mL/min. EE2 was detected by a fluorescence detector at 206 nm (excitation wavelength) and 310 nm (emission wavelength). The mobile phase was 50:50 (v:v) of acetonitrile and deionized water and the flow rate was 1 mL/min. The concentration of PHE was quantified on a fluorescence detector at 250 nm (excitation wavelength) and 364 nm (emission wavelength) for the concentration range of 0.5–50 μg/L, and on a UV detector at 250 nm for the samples with concentrations higher than 50 μg/L. The mobile phase was 90:10 (v:v) of methanol and deionized water for PHE and the flow rate was 0.8 mL/min. Because the loss of solute due to volatilization was negligible, sorbed chemicals were determined by mass difference between initial (C_0) and equilibrated concentrations (C_e). All samples including the blanks were conducted in duplicates.

2.5. Data analysis

In this work, Freundlich model (FM) was used to fit the sorption isotherms:

$$\log q_e = \log K_f + n \log C_e \quad (1)$$

$$K_d = q_e/C_e \quad (2)$$

$$K_{oc} = K_d/f_{oc} \quad (3)$$

where q_e (μg/g) is the equilibrium solid-phase concentration of sorbates, C_e (μg/L) is the equilibrium aqueous concentration, n is the isotherm nonlinearity index, K_f [(μg/g)/(μg/L)^n] is the affinity coefficient of Freundlich model, K_d is the sorption distribution coefficient, and f_{oc} is OC content. The K_{oc} values were calculated at three selected concentrations (C_e = 0.01, 0.1 and 1S_w, water solubility of solutes).

The investigated correlations among properties of sorbents as well as the sorption coefficients of ACE, DBP, EE2 and PHE (Pearson correlation coefficients: P and R^2 values) were obtained from the Pearson correlation analysis by SPSS 16.0 software (SPSS Inc., USA).

3. Results and discussion

3.1. Characteristics of biochars

The PLABs had higher OC contents than ANIBs (Fig. 1a). With increasing HTT, the OC contents of the PLABs increased. However, a similar trend was not observed in ANIBs (Fig. 1a), which can probably be attributed to the relatively higher mineral contents of ANIBs (Table S2, Supplementary data). For all 21 biochars, the polarity index (O/C and (O + N)/C ratios) varied inversely with the HTT (Fig. 1b and Table S2, Supplementary data), indicating a reduction of the polar functional groups and an increase in hydrophobicity (Chen et al., 2008). Moreover, except for those samples at 250 °C, the polarity (O/C and (O + N)/C ratios) of ANIBs was higher than PLABs (Fig. 1b and Table S2, Supplementary data). This may result from the minerals within ANIBs protecting the polar functional groups of OM from being removed during the pyrolysis process (Qiu et al., 2014).

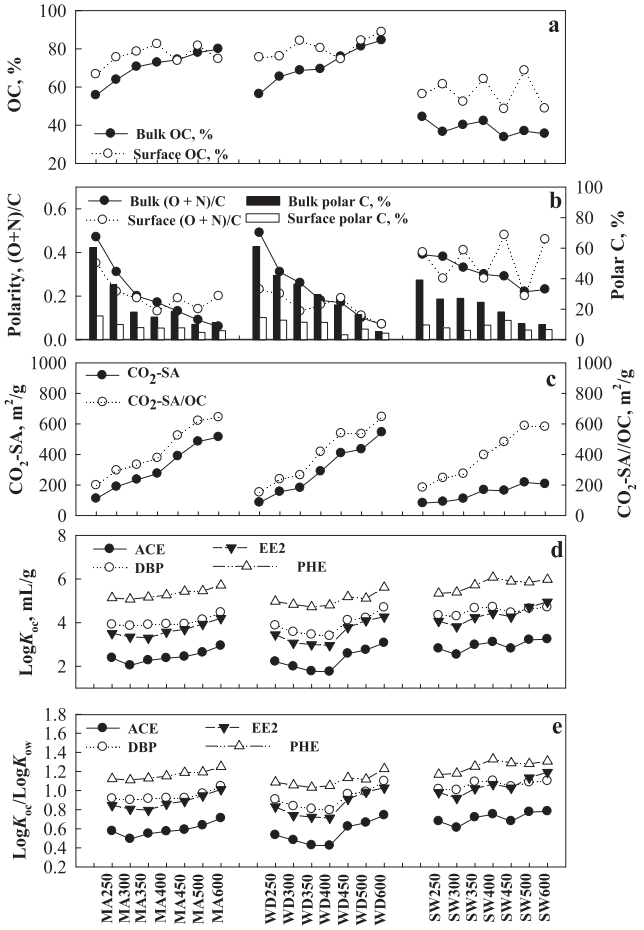

Fig. 1. Comparison of bulk and surface organic carbon (OC) content (**a**); bulk and surface polarity ((O + N)/C) (**b**); bulk and surface polar C content (**b**); surface area determined by CO_2 adsorption (CO_2-SA) (**c**); the OC-normalized CO_2-SA (CO_2-SA/OC) (**c**); OC-normalized distribution coefficients (logK_{oc}) (**d**) and octanol/water distribution coefficient (logK_{ow})-normalized logK_{oc} (logK_{oc}/logK_{ow}) (**e**) among these three kinds of biochars produced from maize straw (MABs), wood dust (WDBs) and swine manure (SWBs), respectively. The connection of the data points by lines in above figure has no specific meaning but indicate the changing trends of biochars as the heat treatment temperature increased. (Bulk polar C: 45–93 ppm + 165–220 ppm; Surface polar C: surface C–O + surface C=O + surface COO).

The bulk elemental compositions of the initial feedstock and the resulting biochars were further analyzed using a van Krevelen diagram, plotting the atomic ratios H/C versus O/C (Fig. 2). The straight lines represent changes in the ratios due to dehydration, decarboxylation, and demethylation processes. High ratios imply the presence of primary plant macromolecules (i.e., cellulose), whereas low ratios are typical of more condensed (aromatic) structures (Cao et al., 2013). SW feedstock had H/C and O/C ratios much higher than MA and WD feedstocks (Fig. 2), which was close to that of cellulose. Moreover, the H/C and O/C ratios of SWBs exhibited smaller variations compared to MABs and WDBs (Fig. 2). As illustrated in Fig. 2, the conversion of SW, MA and WD feedstocks with the increasing HTTs is predominantly governed by the dehydration process (lower H/C ratio) and, from 250 °C to 300 °C, a shift in the O/C ratio of SWBs suggests a demethylation process took place, which did not occur with the MABs and WDBs.

The determination of surface functionalities by the XPS analysis exposed obvious differences between the surface and bulk elemental composition of tested biochars (Table S2 and S3, Supplementary data and Fig. 1a and b). The surface OC of biochars was generally higher than their corresponding bulk OC (Fig. 1a), especially for ANIBs. This result implies that OC may be mainly concentrated on

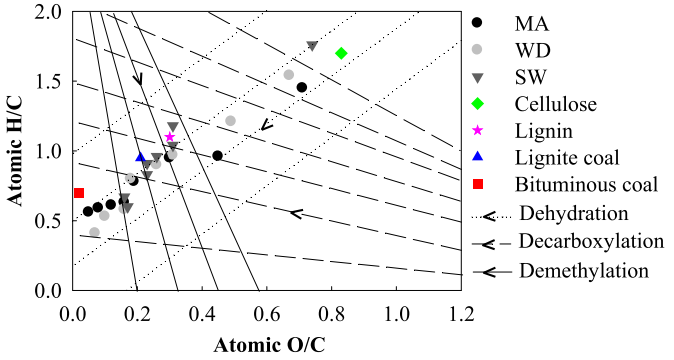

Fig. 2. Atomic H/C and O/C ratios of the feedstocks and biochars derived from maize straw, wood dust and swine manure (MA, WD and SW) produced at different heating treatment temperatures (HTTs). The atomic ratios for cellulose, lignin (Dinjus et al., 2011), and bituminous and lignite coals (Berge et al., 2011) are included for comparative purposes. Note that the points proceed from right to left in the figure in the order of the HTT (0, 250, 300, 350, 400, 450, 500, and 600 °C) for each feedstock material.

the surface of biochar particles, and the minerals within biochars are possibly covered by OM within biochars (Sun et al., 2013). In addition, the surface polarity ((O + N)/C) of all biochars was different from their corresponding bulk polarity (Fig. 1b). Specifically, bulk polarity values of PLABs at low HTTs (≤400 °C) were higher than their corresponding surface values (Fig. 1b), indicating that a higher content of the hydrophobic functionalities in these samples was located on their exterior. In contrast, the reverse was found for PLABs at high HTTs (≥450 °C) (Fig. 1b), which indicates that structural rearrangement may take place in these biochars at high HTTs. The surface polarity values of the ANIBs were higher than those of the PLABs (Fig. 1b), similar to the results found for bulk polarity above. The higher surface polarity of ANIBs (Table S3, Supplementary data) may result partly from their higher ash content, as seen in the significantly positive correlation between the surface polarity of biochars and their ash contents (Fig. S1a, Supplementary data). Moreover, we found that the surface O and surface O/C ratios of ANIBs were positively relevant to their content of surface P or Ca or the sum of surface P and Ca content (Fig. S6b and c, Supplementary data), demonstrating that those minerals containing P and Ca (e.g. calcium phosphates) may be the major sources that contribute to the surface O content of ANIBs.

The ^{13}C NMR spectra patterns (Fig. S2, Supplementary data) of the biochars and the integrated results (Table S4, Supplementary data) show that the structural characteristics of the biochars change greatly during pyrolysis. The contents of O-containing functional groups decreased with increasing HTT (Table S4 and Fig. S2, Supplementary data), which is in line with the decrease in bulk polarity (Fig. 1b). Moreover, the aliphatic C (0–93 ppm) contents of MABs, WDBs and SWBs decreased with increasing HTT, while the aromatic C (93–165 ppm) contents increased remarkably (Table S4, Supplementary data). These results are consistent with previous studies that the molecular structure of biochars transitions from a mainly amorphous characteristic to a crystalline one composed of inorganic ash, microporous voids and turbostratic stacks of rigid graphene sheets with increasing HTT (Keiluweit et al., 2010). When the HTTs were above 450 °C (≥450 °C), all features related to aliphatic C progressively declined, any residual C functionalities diminished and the spectra of these three kinds of biochars became very similar.

It has been previously proposed that with the rise in HTT, graphene-like sheets gradually grow at the expense of amorphous C (Kercher and Nagle, 2003) and since they are often denser than the original amorphous C forms, this conversion eventually leads to the formation of nanopores (D < 2 nm) (Keiluweit et al., 2010). Consistently, CO_2-SA of the test biochars rose with increasing HTT (Table S2, Supplementary data and Fig. 1c). Moreover, the CO_2-SA values of the two kinds of PLABs (110.2–513.4 m^2/g and 85.0–544.6 m^2/g) were remarkably higher than that of the ANIBs (81.0–206.1 m^2/g) at each corresponding HTT. This might be attributed to the higher OC content of PLABs (Table S2, Supplementary data and Fig. 1a), because there was a positive correlation between the CO_2-SA values of all biochars and the OC contents (Fig. S1b, Supplementary data). Nevertheless, the CO_2-SA of biochars is not dominated by their OC content, supported by the incomparable OC-normalized CO_2-SA (CO_2-SA/OC) values of PLABs and ANIBs (Table S2, Supplementary data). Thus there are other factors also regulating the CO_2-SA of biochars. As expected, the CO_2-SA/OC values of all three kinds of biochars were positively related with their aryl-C or aromaticity (Fig. S1c, Supplementary data), but negatively associated with alkyl-C or aliphaticity (Fig. S1d, Supplementary data) and bulk polarity (Fig. S1e, Supplementary data), demonstrating the influence of aromatic structure of biochars on their porosity characteristics (Han et al., 2014).

3.2. *Effect of biochar structure on nonlinearity* n *values*

All the sorption isotherms of ACE, DBP, EE2 and PHE (Fig. S3, Supplementary data) onto the tested biochars and the original feedstocks were fitted well using the Freundlich model. The nonlinearity coefficient (n) values of the original feedstocks were higher than those of the corresponding biochars, whose n values were all less than 1 (Table S5–S8, Supplementary data). The n values of the four sorbates by all three kinds of biochars, excluding the sorption of DBP onto SWBs and the sorption of PHE onto WDBs, were positively correlated with their atomic ratios H/C (Fig. S4a–d, Supplementary data). Generally, the n values were significantly and positively relevant with their bulk polarity (O + N)/C (Fig. S4e–h, Supplementary data), but negatively correlated with aromaticity (Fig. S5a–d, Supplementary data), which is consistent with the report by Zhu and Pignatello (2005) that aromatic domains contribute to nonlinearity. Thus, the increasing nonlinearity of the sorption isotherms of ACE, DBP and EE2 onto these three kinds of biochars and PHE onto MABs and SWBs with the increasing HTT (Table S5–S8, Supplementary data) is linked to the rising aromaticity and decreasing H/C and polarity of biochars with the increasing HTT (Pignatello and Xing, 1995; Ran et al., 2007). As discussed in the previous section, the changes in these factors corresponded to an increase in biochar microporosity as measured by CO_2-SA/OC values. Additionally, it has been commonly accepted that the microporosity of organic sorbents gives rise to isotherm nonlinearity (Pignatello and Xing, 1995), which was also seen here with the negative correlation between n and CO_2-SA/OC (Fig. S5e–h, Supplementary data).

3.3. *The impact of heating treatment temperatures and feedstocks on the sorption capacity (logK_{oc}) of biochars*

In general, higher HTT increased the sorption capacity for all biochars and compounds (Fig. 1d). This agrees with results from previous studies that higher HTT biochars are more effective in sorption and sequestration of organic contaminants in soils (Chun et al., 2004; Chen et al., 2008). However, the increase in logK_{oc} with increasing HTT is not uniform for WDBs and SWBs. For example, while the highest logK_{oc} values for the sorption of ACE and EE2 onto SWBs were at 600 °C, SW400 had the highest logK_{oc} values for DBP and PHE (Fig. 1d). This can probably be attributed to the higher number of polar functional groups in LTBs, which can be involved in interactions via specific adsorption including H-bonding and π–π interactions (Sun et al., 2013). This is consistent with our

previous studies on the sorption of PAEs and herbicides by biochars (Sun et al., 2011a, 2012).

Among these three kinds of biochars, the SWBs demonstrated the highest logK_{oc} values (C_e = 0.01 S_w) of all sorbates (Fig. 1d), indicating that it is a more promising sorbent for environmental applications than MABs and WDBs. The positive relationship between logK_{oc} values of all the biochars and their ash contents (Fig. S6a, Supplementary data) suggests that the high capacity of SWBs is probably due to their ash content.

For the low ash PLABs, MABs with the higher ash content (except at 400 °C) tended to have greater logK_{oc} values (C_e = 0.01 S_w) than WDBs for the sorption of ACE, DBP and EE2 when the HTTs were low (≤400 °C) (Fig. 1d). And above 450 °C (≥450 °C), it was reversed. For PHE, the MABs logK_{oc} values were higher than the WDBs for all HTTs (Fig. 1d). Further physical and chemical differences between the biochars, for example the CO_2-SA/OC, may account for the above results. The relationships between logK_{oc} values and CO_2-SA/OC values were positive for the sorption of all four kinds of sorbates onto WDBs ($p < 0.05$ for ACE, DBP and EE2; $p < 0.01$ for PHE) and the PHE onto MABs ($p < 0.05$ for PHE) (Fig. 3a and b). Thus, generally the higher sorption capacity of MABs at low HTTs corresponds to their higher CO_2-SA/OC values than those of WDBs, while the higher CO_2-SA/OC values of the WDBs at high HTTs led to higher logK_{oc} values (Table S2, Supplementary data). An additional factor that plays a role is the aromaticity of the biochars, which could contribute to sorption through π–π interactions with the sorbates. The higher aromaticity of the MABs except for 450 °C (Table S4, Supplementary data) may explain the different behavior of PHE that logK_{oc} for PHE of MABs was higher for all HTTs.

3.4. Roles of polarity, aliphatic and aromatic C in sorption of each given sorbate by biochars

Generally, the order of increasing logK_{oc} (C_e = 0.01 S_w) values followed the hydrophobicity of sorbates for the three kinds of biochars: PHE (octanol/water distribution coefficient (logK_{ow}) = 4.57) > DBP (logK_{ow} = 4.27) > EE2 (logK_{ow} = 4.15) > ACE (logK_{ow} = 4.14) (Table S5–S8, Supplementary data), which highlights the significance of the hydrophobic effect. However, further sorption mechanisms are involved due to the incomparable values of normalized logK_{oc} by logK_{ow} (logK_{oc}/logK_{ow}) (Table S9, Supplementary data and Fig. 1e), since if the sorption was only attributed to hydrophobic partition, the obtained logK_{oc}/logK_{ow} values should be comparable (Sun et al., 2011b).

Previous studies showed that H-bonding interaction could occur especially for sorbates and sorbents with polar functional groups (Crittenden et al., 1999). The O atoms of ACE and DBP could act as H-bonding acceptors and EE2 is able to serve as both H-bonding acceptor and H-bonding donor (Sun et al., 2012). Though the PHE molecule doesn't have any H-bonding acceptor or donor atom, it has been reported that the rings of PHE could act as a weak H-bonding acceptor due to the absence of hydroxyl group (Zhu et al., 2004). The numerous O-containing functional groups and N-contents of the LTBs could have a high potential as H-bonding accepter or donor. Thus, it is reasonable to speculate that the tested sorbate can be adsorbed by LTBs (HTTs ≤ 400 °C) through H-bonding interactions or π-H bonding (Zhu et al., 2004). This is confirmed by the significantly positive correlations observed between logK_{oc} values of all sorbates and the surface polarity of LTBs ($p < 0.01$ for ACE, DBP, and EE2; $p < 0.05$ for PHE) (Fig. 3d). In addition, DBP and EE2, which possess more H-bonding sites (Table S1, Supplementary data), had higher sorption capacities on the biochars than ACE. However, as the polarity of LTBs declined with the increasing HTT, the logK_{oc} of LTBs did not follow the same trend except for the LTBs-WDBs (Fig. 1d), implying that there would be other factors regulating the sorption ability of LTBs-MABs and LTBs-SWBs. Moreover, the logK_{oc} values of DBP and EE2 by the LTBs-WDBs (≤400 °C) were positively correlated with their aliphaticity ($p < 0.05$ for DBP and EE2) (Fig. 3e). Additionally, the logK_{oc} values of ACE and PHE generally were declined as the aliphaticity of the LTBs-WDBs (≤400 °C) decreased with increasing HTT (Table S4, S5 and S8, Supplementary data). These indicate that the sorption of the solutes by LTBs-WDBs is also dependent on their aliphatic C domains. And since the reduction of aliphaticity was as a result of the increasing HTTs, these could probably explain why the logK_{oc} values of these sorbates on LTBs-WDBs (≤400 °C) decreased with the increasing HTT.

In contrast, for the biochars produced at relatively high HTTs (≥450 °C), the logK_{oc} values of the sorbates correlated positively with the aromaticity of biochars ($p < 0.01$ for ACE, DBP, and EE2; $p < 0.05$ for PHE) (Fig. 3f). So with the increasing HTT, aromatic moieties become the dominant sorption domains for these sorbates rather than aliphatic moieties. There are probably two reasons for this. 1) The residue aliphatic domains of the HTBs could be masked by the condensed domains, and thus might be inaccessible for the compounds. With increasing HTT, the aliphatic C contents decreased dramatically, and the molecular structure of biochars gradually changed into crystalline material with rigid graphene sheets (Keiluweit et al., 2010). The condensed domains may therefore reduce the accessibility of the sorbates to aliphatic domains. It was proposed that the alignment of crystalline subdomains in semicrystalline polymers could affect the availability of the amorphous domains for HOCs sorption (Hale et al., 2011). 2) The larger graphene sheets in biochars could be available for the sorbates via π–π electron–donor–acceptor (EDA) interactions. The EDA interaction is a specific, noncovalent attractive force that exists between electron-rich (π-donor) and -poor (π-acceptor) arenas (Wang and Xing, 2007). Previous studies have indicated that the biochars generated at intermediate energy may be bipolar; aromatic rings in the center of a given sheet are electron deficient, and carbon rings closer to the edges are left electron rich (Sun et al., 2012; Zhu and Pignatello, 2005). Moreover, PHE can behave as donor, while ACE, DBP, and EE2 can act as π-acceptors because their benzene rings are electron-deficient. Therefore, π–π EDA interactions between the biochar and the sorbates could be expected.

Apart from H-bonding and π–π EDA interaction, Chun et al. (2004) has reported that pore-filling is one of the dominant mechanisms for HOCs sorption to pyrolyzed chars. There were positive correlations between logK_{oc} values and the CO_2-SA/OC for all the sorbates onto WDBs ($p < 0.05$ for ACE, DBP and EE2; $p < 0.01$ for PHE) (Fig. 3a). Although this correlation was not observed in the sorption of ACE and DBP onto SWBs ($p < 0.05$ for EE2 and PHE) and for MABs it only existed in the sorption of PHE ($p < 0.05$ for PHE) (Fig. 3b and c), the n of these sorption isotherms of ACE, EE2, PHE, and DBP were generally correlated inversely with the CO_2-SA/OC of all investigated biochars (Fig. S5e–h, Supplementary data). Based on our analysis, CO_2-SA/OC (ie. pore-filling) may be one of the additional factors responsible for the sorption of these biochars.

4. Conclusion

The properties of biochars vary dramatically with HTTs and feedstock sources, and thus significantly impact their sorption capacity for HOCs. Among the four sorbates investigated in our study, the logK_{oc} values followed the order of the hydrophobicity of sorbates. The SWBs, the biochars with the highest ash contents, showed higher sorption capacity than the PLABs. Of the two kinds of PLABs, we found that MABs tended to have relatively larger logK_{oc} values than WDBs when the HTTs were low, probably due

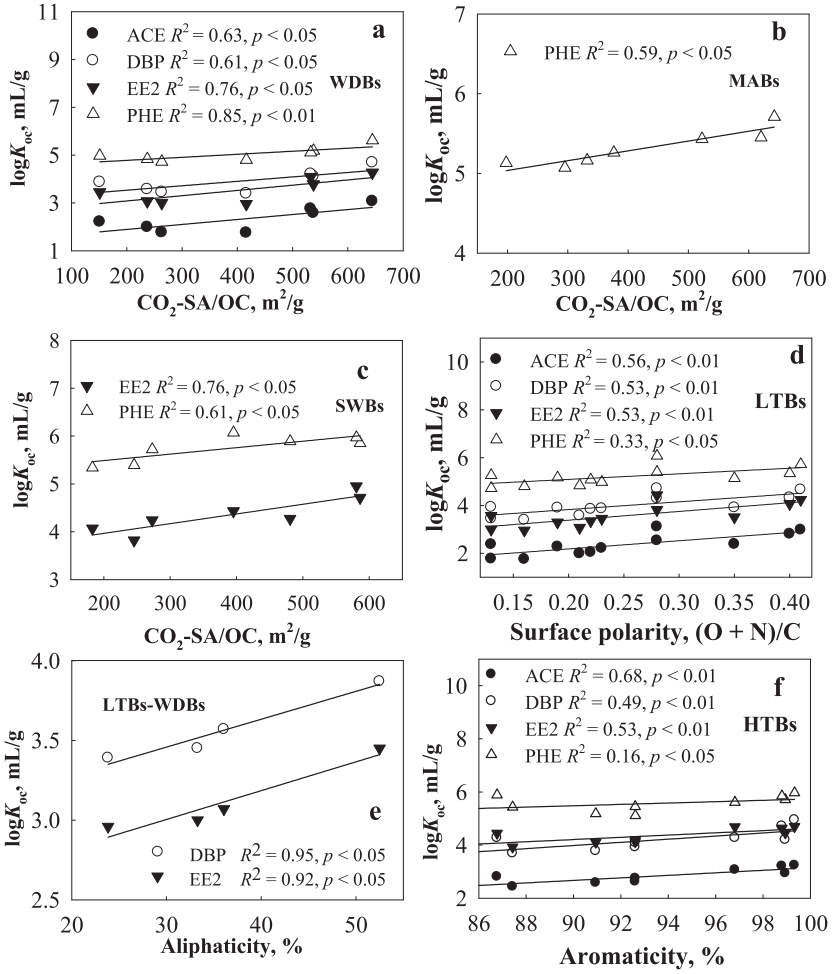

Fig. 3. Relationships between organic carbon (OC)-normalized sorption distribution coefficients ($\log K_{oc}$) of sorbates and OC-normalized surface area determined by CO_2 adsorption (CO_2-SA/OC) of wood dust biochars (WDBs) (**a**), maize straw biochars (MABs) (**b**) and swine manure biochars (SWBs) (**c**), between $\log K_{oc}$ and the surface polarity ((O + N)/C) of biochars charred at ≤ 400 °C (LTBs) (**d**), between $\log K_{oc}$ of DBP and EE2 and the aliphaticty of biochars charred ≤ 400 °C (LTBs) (**e**), between $\log K_{oc}$ and the aromaticity of biochars charred at ≥ 450 °C (HTBs) (**f**). Note that LTBs-WDBs represents the biochars obtained from wood dust at ≤ 400 °C.

to the higher CO_2-SA/OC, ash content and aromaticity of MABs. Furthermore, our results indicate that different sorption mechanism may take place between LTBs and HTBs: H-bonding and the aliphatic domains may regulate the sorption of WDBs obtained at relatively low HTTs (≤400 °C), while aromatic C affects the sorption of biochars at high HTTs. Pore-filling may be one of the additional factors responsible for the sorption of these biochars. The results of our study contribute to the understanding of the effect of feedstocks sources and the HTTs on the chemical and physical properties of biochars, and more importantly, can provide a theoretical basis for the efficient use of biochars in environmental applications as sorbents.

Acknowledgments

This research was supported by the Fund for Innovative Research Group of the National Natural Science Foundation of China (51421065), National Natural Science Foundation of China (41273106), USDA Hatch Program (MAS 00982), Beijing Higher Education Young Elite Teacher Project, and the Scientific Research Foundation for the Returned Overseas Chinese Scholars, State Education Ministry. Mention of trade names or commercial products is solely for the purpose of providing specific information and does not imply recommendation or endorsement by the U.S. Department of Agriculture.

Appendix A. Supplementary data

Supplementary data related to this article can be found at http://dx.doi.org/10.1016/j.chemosphere.2015.08.042.

References

Berge, N.D., Ro, K.S., Mao, J., Flora, J.R., Chappell, M.A., Bae, S., 2011. Hydrothermal carbonization of municipal waste streams. Environ. Sci. Technol. 45, 5696–5703.
Braida, W.J., Pignatello, J.J., Lu, Y., Ravikovitch, P.I., Neimark, A.V., Xing, B., 2003. Sorption hysteresis of benzene in charcoal particles. Environ. Sci. Technol. 37, 409–417.
Cao, X., Ro, K.S., Libra, J.A., Kammann, C.I., Lima, I., Berge, N., Li, L., Li, Y., Chen, N., Yang, J., 2013. Effects of biomass types and carbonization conditions on the chemical characteristics of hydrochars. J. Agric. Food Chem. 61, 9401–9411.
Chen, B., Zhou, D., Zhu, L., 2008. Transitional adsorption and partition of nonpolar and polar aromatic contaminants by biochars of pine needles with different pyrolytic temperatures. Environ. Sci. Technol. 42, 5137–5143.
Chen, Z., Chen, B., Chiou, C.T., 2012. Fast and slow rates of naphthalene sorption to biochars produced at different temperatures. Environ. Sci. Technol. 46, 11104–11111.
Chun, Y., Sheng, G., Chiou, C.T., Xing, B., 2004. Compositions and sorptive properties of crop residue-derived chars. Environ. Sci. Technol. 38, 4649–4655.
Crittenden, J.C., Sanongraj, S., Bulloch, J.L., Hand, D.W., Rogers, T.N., Speth, T.F., Ulmer, M., 1999. Correlation of aqueous-phase adsorption isotherms. Environ. Sci. Technol. 33, 2926–2933.
Dinjus, E., Kruse, A., Troeger, N., 2011. Hydrothermal carbonization–1. Influence of lignin in lignocelluloses. Chem. Eng. Technol. 34, 2037–2043.
Hale, S.E., Cornelissen, G., Arp, H.P.H., 2011. Comment on "partition coefficients of organic contaminants with carbohydrates". Environ. Sci. Technol. 45 1158–1158.

Han, L., Sun, K., Jin, J., Wei, X., Xia, X., Wu, F., Gao, B., Xing, B., 2014. Role of structure and microporosity in phenanthrene sorption by natural and engineered organic matter. Environ. Sci. Technol. 48, 11227–11234.
Keiluweit, M., Nico, P.S., Johnson, M.G., Kleber, M., 2010. Dynamic molecular structure of plant biomass-derived black carbon (biochar). Environ. Sci. Technol. 44, 1247–1253.
Kercher, A.K., Nagle, D.C., 2003. Microstructural evolution during charcoal carbonization by X-ray diffraction analysis. Carbon 41, 15–27.
Lehmann, J., Gaunt, J., Rondon, M., 2006. Bio-char sequestration in terrestrial ecosystems–a review. Mitig. Adapt. Strat. Gl. 11, 395–419.
Novak, J.M., Lima, I., Xing, B., Gaskin, J.W., Steiner, C., Das, K., Ahmedna, M., Rehrah, D., Watts, D.W., Busscher, W.J., 2009. Characterization of designer biochar produced at different temperatures and their effects on a loamy sand. Annu. Environ. Sci. 3, 195–206.
Pignatello, J.J., Xing, B., 1995. Mechanisms of slow sorption of organic chemicals to natural particles. Environ. Sci. Technol. 30, 1–11.
Qiu, M., Sun, K., Jin, J., Gao, B., Yan, Y., Han, L., Wu, F., Xing, B., 2014. Properties of the plant-and manure-derived biochars and their sorption of dibutyl phthalate and phenanthrene. Sci. Rep. 4.
Ran, Y., Sun, K., Yang, Y., Xing, B., Zeng, E., 2007. Strong sorption of phenanthrene by condensed organic matter in soils and sediments. Environ. Sci. Technol. 41, 3952–3958.
Sohi, S., Krull, E., Lopez-Capel, E., Bol, R., 2010. A review of biochar and its use and function in soil. Adv. Agron. 105, 47–82.
Sun, K., Jin, J., Keiluweit, M., Kleber, M., Wang, Z., Pan, Z., Xing, B., 2012. Polar and aliphatic domains regulate sorption of phthalic acid esters (PAEs) to biochars. Bioresour. Technol. 118, 120–127.
Sun, K., Kang, M., Zhang, Z., Jin, J., Wang, Z., Pan, Z., Xu, D., Wu, F., Xing, B., 2013. Impact of deashing treatment on biochar structural properties and potential sorption mechanisms of phenanthrene. Environ. Sci. Technol. 47, 11473–11481.
Sun, K., Keiluweit, M., Kleber, M., Pan, Z., Xing, B., 2011a. Sorption of fluorinated herbicides to plant biomass-derived biochars as a function of molecular structure. Bioresour. Technol. 102, 9897–9903.
Sun, K., Ro, K., Guo, M., Novak, J., Mashayekhi, H., Xing, B., 2011b. Sorption of bisphenol A, 17α-ethinyl estradiol and phenanthrene on thermally and hydrothermally produced biochars. Bioresour. Technol. 102, 5757–5763.
Wang, X., Xing, B., 2007. Sorption of organic contaminants by biopolymer-derived chars. Environ. Sci. Technol. 41, 8342–8348.
Yang, Y., Shu, L., Wang, X., Xing, B., Tao, S., 2011. Impact of de-ashing humic acid and humin on organic matter structural properties and sorption mechanisms of phenanthrene. Environ. Sci. Technol. 45, 3996–4002.
Zhu, D., Hyun, S., Pignatello, J.J., Lee, L.S., 2004. Evidence for π–π electron donor–acceptor interactions between π-donor aromatic compounds and π-acceptor sites in soil organic matter through pH effects on sorption. Environ. Sci. Technol. 38, 4361–4368.
Zhu, D., Pignatello, J.J., 2005. Characterization of aromatic compound sorptive interactions with black carbon (charcoal) assisted by graphite as a model. Environ. Sci. Technol. 39, 2033–2041.